

Immunosuppressive Drug Resistant Armored TCR T cells for immune-therapy of HCC in liver transplant patients

Morteza Hafezi^{1,2}, Meiyin Lin^{1,3}, Adeline Chia¹, Alicia Chua⁴, Zi Zong Ho⁴, Royce Fam⁴, Damien Tan³, Joey Aw³, Andrea Pavesi³, Thinesh Lee Krishnamoorthy⁵, Wan Cheng Chow⁵, Wenjie Chen⁶, Qi Zhang⁶, Lu-En Wai^{4,7}, Sarene Koh^{4,7}, *Anthony T. Tan¹, *Antonio Bertoletti^{1,7}.

This article has been accepted for publication and undergone full peer review but has not been through the copyediting, typesetting, pagination and proofreading process, which may lead to differences between this version and the [Version of Record](#). Please cite this article as [doi: 10.1002/HEP.31662](#)

This article is protected by copyright. All rights reserved



Background & Aims: HBV-specific T cell receptor (HBV-TCR) engineered T cells have the potential for treating hepatocellular carcinoma (HCC) relapses after liver transplantation, but their efficacy can be hampered by the concomitant immunosuppressive treatment required to prevent graft rejection. Our aim is to molecularly engineer TCR-T cells that could retain their polyfunctionality in such patients while minimising the associated risk of organ rejection.

Approach & Results: We first analysed how immunosuppressive drugs can interfere with the in vivo function of TCR-T cells in liver transplanted patients with HBV-HCC recurrence receiving HBV-TCR T cells, and in vitro in the presence of clinically relevant concentrations of immunosuppressive Tacrolimus (TAC) and Mycophenolate Mofetil (MMF). Immunosuppressive Drug Resistant Armored (IDRA) TCR-T cells of desired specific (HBV or EBV) were then engineered by concomitantly electroporating mRNA encoding specific-TCRs and mutated variants of calcineurin B (CnB) and inosine-5'-monophosphate dehydrogenase (IMPDH), and their function was assessed through intracellular cytokine staining and cytotoxicity assays in the presence of TAC and MMF.

Liver transplanted HBV-HCC patients receiving different immunosuppressant drugs exhibited varying levels of activated (CD39+ Ki67+) PBMCs post HBV-TCR T cell infusions that positively correlates with clinical efficacy. In vitro experiments with TAC and MMF showed a potent inhibition of TCR-T cell polyfunctionality. This inhibition can be effectively negated by the transient overexpression of mutated variants of CnB and IMPDH. Importantly, the resistance only lasted for 3-5 days after which sensitivity was restored.

Conclusions: We engineered TCR-T cells of desired specificities that transiently escape the immunosuppressive effects of TAC and MMF. This finding has important clinical applications for the treatment of HBV-HCC relapses and other pathologies occurring in organ transplanted patients.



Ability of HBV-TCR-T cells treatment to modify immunological profile in patients

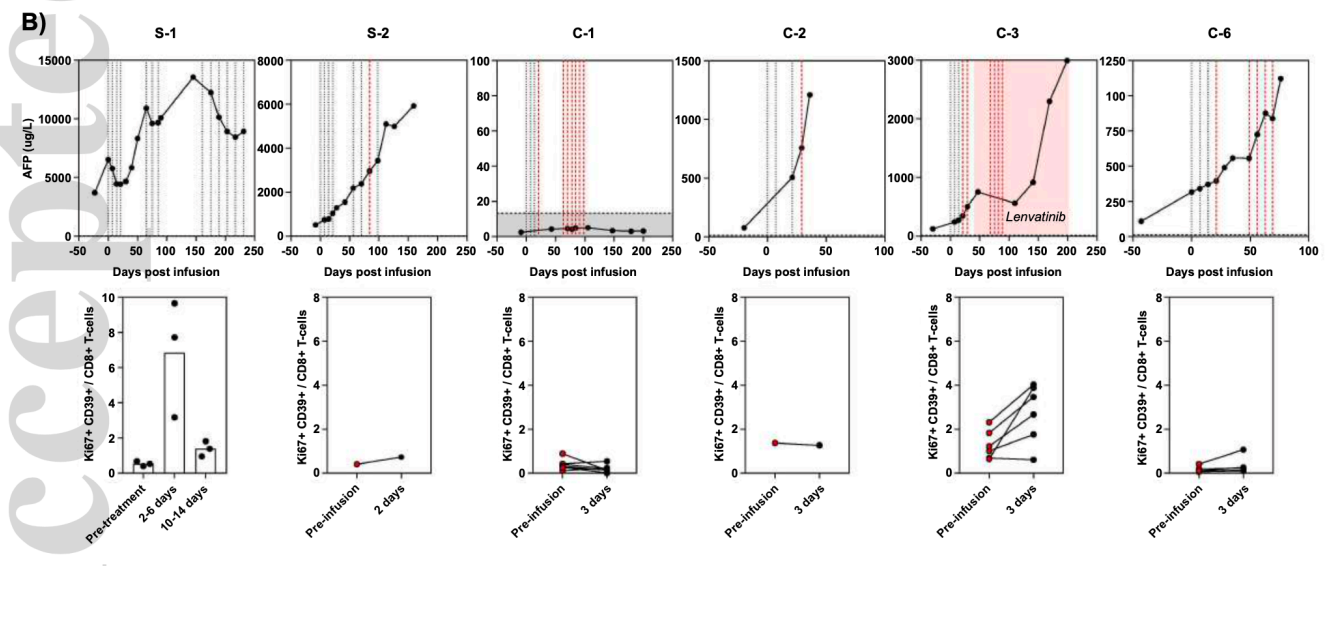
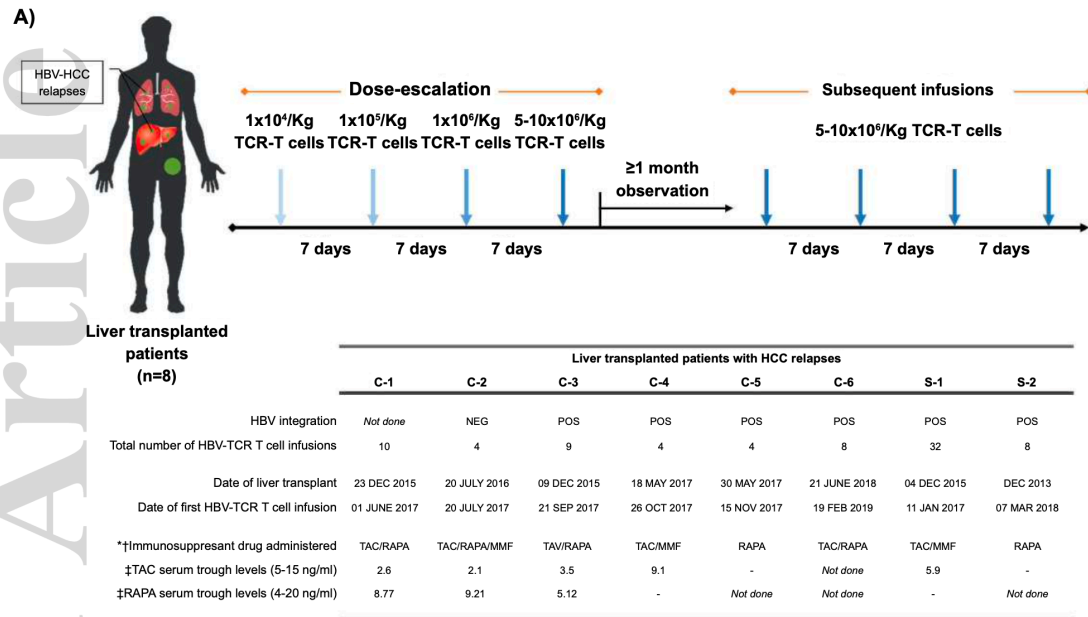
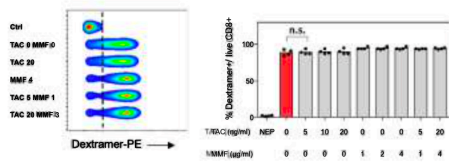


Fig. 1. Alterations of the peripheral blood immunological profile in liver transplanted HBV-HCC patients treated with HBV-TCR T cells. (A) Schematic illustrates the infusion dose and schedule of liver transplanted HBV-HCC patients treated with mRNA electroporated HBV-TCR T cells (n=8). All patients received 4 escalating doses of HBV-TCR T cells before subsequent infusions of 5- 10x10⁶/Kg HBV-TCR T cells commence. The table details the clinical information and different immunosuppressant regimens that the patients received following liver transplantation. (B) Phenotypic analysis of PBMCs collected from patients before and after receiving HBV-TCR T cells (n=6). Serum AFP levels were monitored before and throughout the treatment (top row). Each dotted line denotes a single infusion of HBV-TCR T cells. Reference range of serum AFP are shown in grey. The frequency of Ki67+ CD39+ CD8 T cells before and after HBV-TCR T cell infusions are shown below. The red circles corresponds to the pre-infusion samples obtained at the time points denoted by the red dotted lines. Patient C-3 received concurrent Lenvatinib treatment for the duration shown (red).

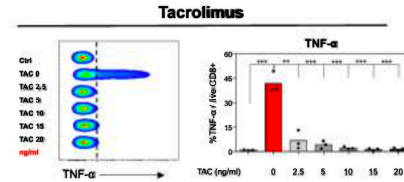


Differential effects of immunosuppressive drugs on engineered HBV-TCR T cells

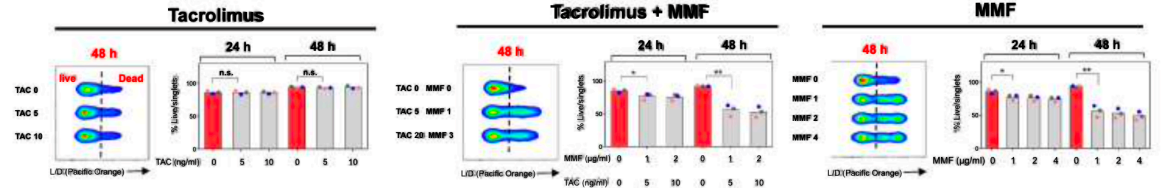
A) TCR expression



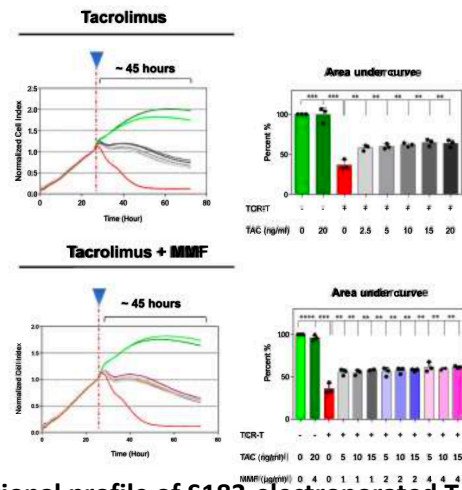
B) Intracellular cytokine production



D) T cell viability



C) Real-time killing assay



E) 3-D Microdevice (T cell migration and function)

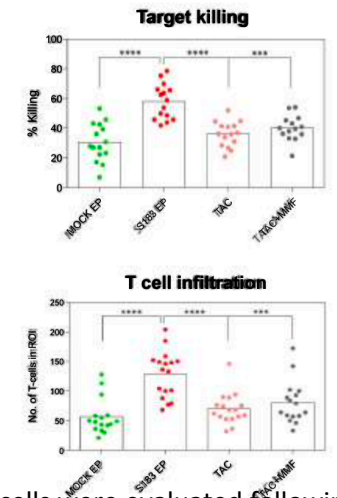
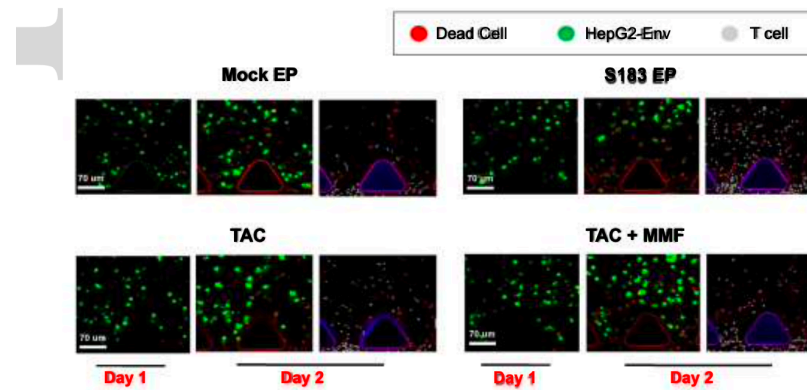
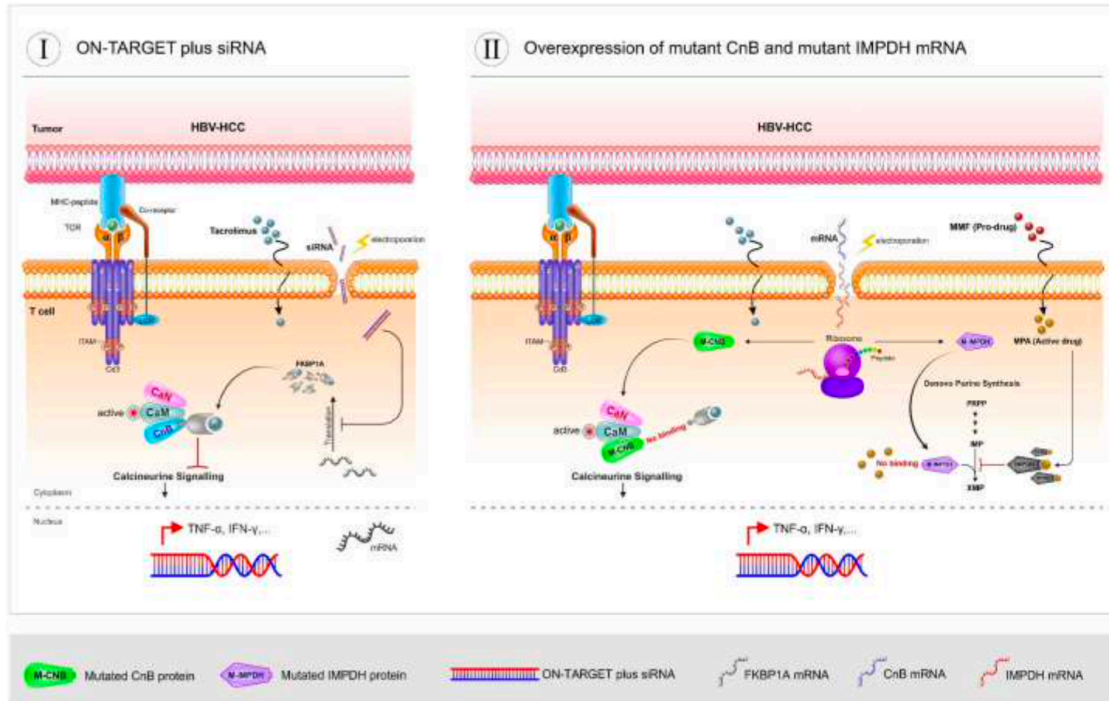


Fig. 2. Functional profile of S183-electroporated T cell treated with clinically relevant concentrations of immunosuppressive drugs. (A) TCR expression of S183 TCR-T cells were evaluated following 24 hours of IS drug treatment. Representative experiment stained for S183- specific TCR (left panel). Percentage of dextramer positive cells out of total live CD8+ T cells were quantified following incubation with the drug (n=3). (B) IS drug treated S183 TCR-T cells were co- cultured with HepG2.215 cells overnight and the frequency of TNF- α -producing CD8+ cells (right panel) out of total live CD8+ T cells were quantified (n=3). Representative experiment stained for TNF- α production (left panel). DMSO-treated T cells cultured without targets served as negative control. (C) T cell cytolysis determined by real-time killing assay in the presence or absence of the drugs. Normalized Cell Index plot (left panel) for HepG2.215 cells with/without drug treated T cell at E: T ratio of 1:1. All samples have been internally normalized for the cell index value measured before T cell addition (indicated by the vertical red dash line). Bar graphs (right panel) demonstrate percentage of T cell cytolysis up to 45 hours after S183-TCR-T cell addition to the targets. (D) Drug impact on T cell viability were analysed at different time point using flow cytometry. Representative experiment stained with live/dead discrimination dye (left panel). (E) Representative images of 3D experiment in various conditions. Engineered T cells labelled with BMQC were introduced into a 3D microdevice in the presence of 5ng/ml of Tacrolimus and DRAQ7. Target death was quantified by measuring DRAQ7 positive cells after the indicated time. Scale bar: 80 μ m. T cell infiltration into the matrix gel was evaluated at the end of the experiment in each respective condition. Each dot (gray) represents the localization of a single T cell in the gel matrix. In all experiments, each dot represents one individual experiment in the bar graphs. Statistical significance was evaluated by either one-way ANOVA followed by Turkey multiple or 2-tailed t test comparison test (*0.01 to 0.05, ** 0.001 to 0.01, *** 0.0001 to 0.001, **** < 0.0001, n.s., not significant).

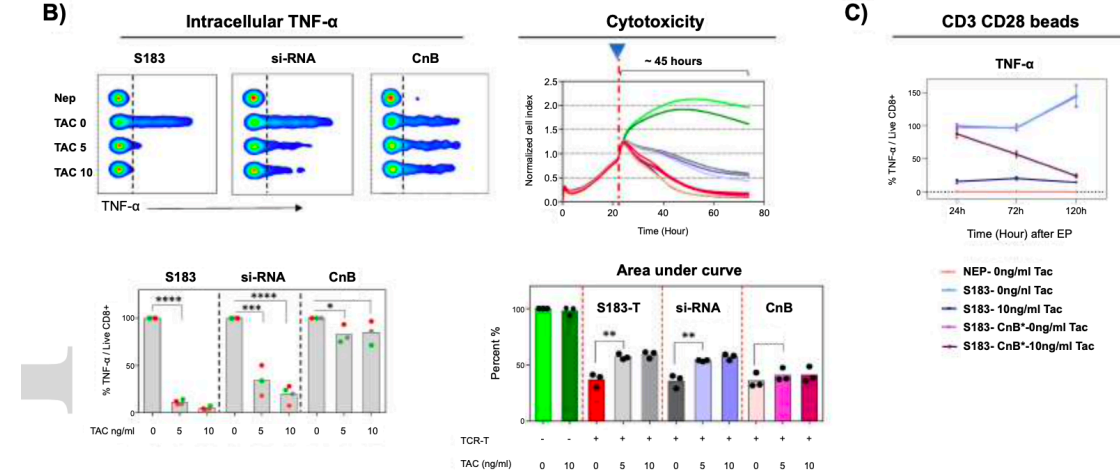


IDRA TCR -T cells engineered through transient overexpression of mutant CnB and IMPDH

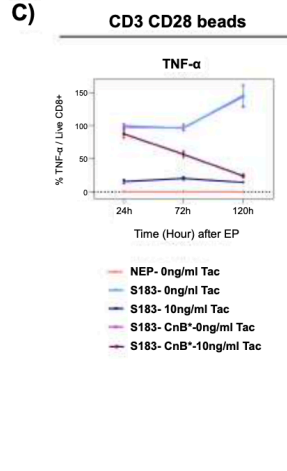
A)



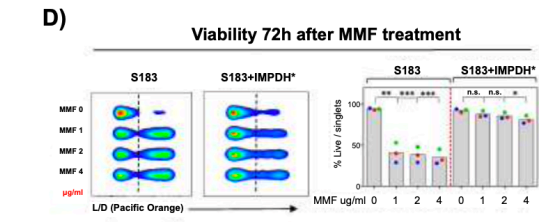
B)



C)



D)



E)

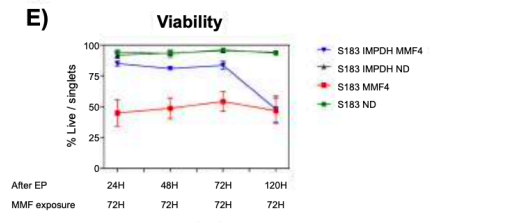


Fig. 3. mRNA electroporation have superior advantage over siRNA for developing IDRA TCR-T cells. (A) Strategies to engineer IDRA TCR-redirection T cells. Schematic illustrating the methods to develop transient IDRA TCR T cells. 1: Targeting FKBP1A mRNA using smart target pool siRNA. 2: Electroporating mRNA encoding mutant CnB and mutant IMPDH. (B) Frequency of TNF- α -producing CD8⁺ cells out of total live CD8⁺ T cells were quantified following overnight incubation with HepG2.215 targets (n=3). Representative experiment stained for TNF- α production (left panel). DMSO-treated T cells without targets served as negative control. T cell cytotoxicity determined by real-time killing assay in the presence and absence of both drugs (right panel). Bar graphs demonstrate percentage of T cell cytotoxicity up to 45 hours after TCR T cell addition to the targets. (C) Evaluation of the kinetics of immunosuppressant drug resistance in an antigen independent (CD3 CD28 activation) manner. (D) Viability of IMPDH electroporated T cells evaluated 72 hours after exposure to clinically relevant concentrations of MMF. Representative experiment stained with live/dead discrimination dye (left panel). (E) Longitudinal viability analysis of IMPDH electroporated T cells. In all experiments, each dot represents one individual experiment in bar graphs. Statistical significance was evaluated by 2-tailed t test (*0.01 to 0.05, ** 0.001 to 0.01, *** 0.0001 to 0.001, **** < 0.0001, n.s., not significant).



IDRA TCR -T cells engineered through transient overexpression of mutant CnB and IMPDH

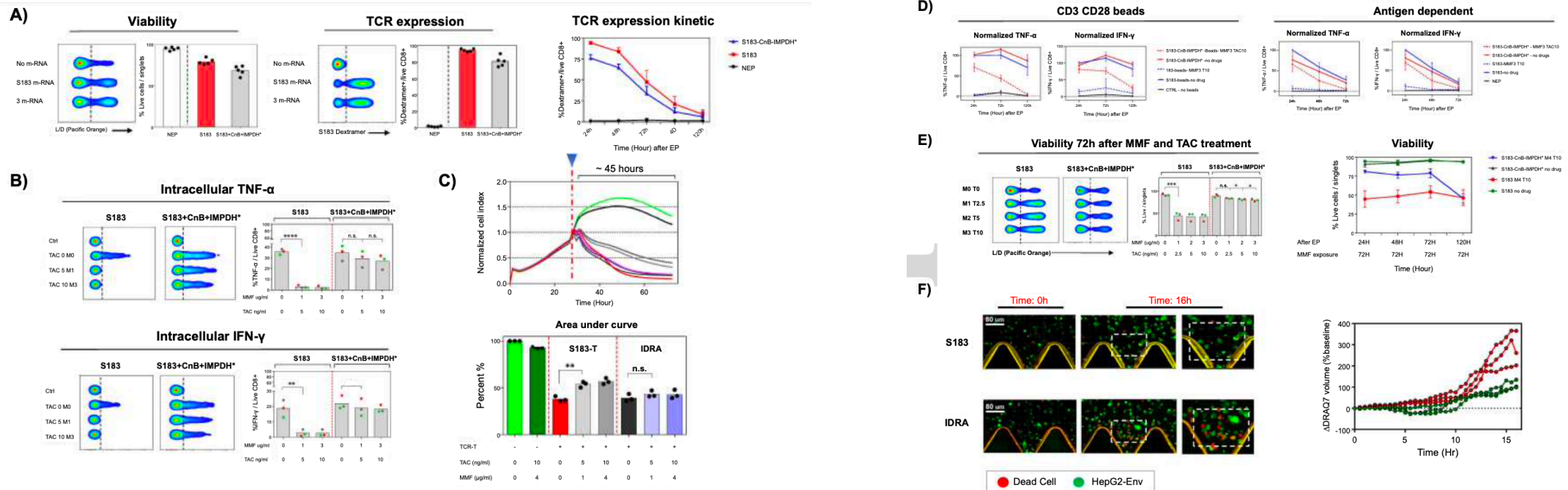


Fig. 4. Developing dual-resistant TCR-directed T cells for liver transplants under MMF and Tacrolimus combination. To develop dual-resistant T cells, all 3 mRNAs including env-s183, mutant CnB and IMPDH were concomitantly electroporated to the T cells. (A) Viability, TCR expression and TCR kinetic of IDRA-T cells evaluated post electroporation. Non-electroporated T cells used as a negative control in the experiments. (B) Frequency of IFN- γ and TNF- α -producing CD8+ cells out of total live CD8 T cells were quantified following overnight incubation with the HepG2.215 targets (n=3). Representative experiment stained for TNF- α and IFN- γ production. DMSO-treated T cells without targets served as negative control. (C) T cell cytolysis determined by real time killing assay in the presence and absence of both drugs. Bar graphs demonstrate percentage of T cell cytolysis up to 45 hours after TCR-T cell addition to the targets. (D) Kinetic analysis of IDRA T cells function in both antigen independent (Anti CD3 CD28 dynabeads) (left panel) and antigen dependent (target: hepG2.2.15) (right panel) manner. (E) Viability of dual resistant TCR-T cells evaluated 72 hours after exposure to clinically relevant concentration of both drugs (left panel). Density plots shows a representative experiment stained with live/dead discrimination dye. Longitudinal viability analysis of dual resistant IDRA TCR-T cells (right panel). In all experiments, each dot represents one individual experiment in bar graphs. (F) Engineered T cells were labelled with BMQC and introduced into 3D microdevice in the presence of 5ng/ml of Tacrolimus and DRAQ7. Target death was quantified by measuring DRAQ7 positive cells at ~30min interval for ~16hours (right panel). Representative images acquired at the indicated times are shown (left panel). Scale bar: 80 μ M. Statistical significance was evaluated by either one-way ANOVA followed by Turkey multiple or 2-tailed t test comparison test (*0.01 to 0.05, ** 0.001 to 0.01, *** 0.0001 to 0.001, **** < 0.0001, n.s., not significant). (G) CD39 and Ki67 phenotypic analysis of conventional and IDRA HBV-TCR T cells after 24hr exposure to TAC and MMF. Density plots shows a representative experiment where the frequency of CD39+ Ki67+ T cells out of total live T cells are indicated. Bar graph summarises two independent experiments and the frequency of CD39+ Ki67+ T cells were normalised to the control where cells were cultured without immunosuppressant drugs.



Engineering of IDRA TCR T cells specific for viral pathologies occurring in IS drug treated patients

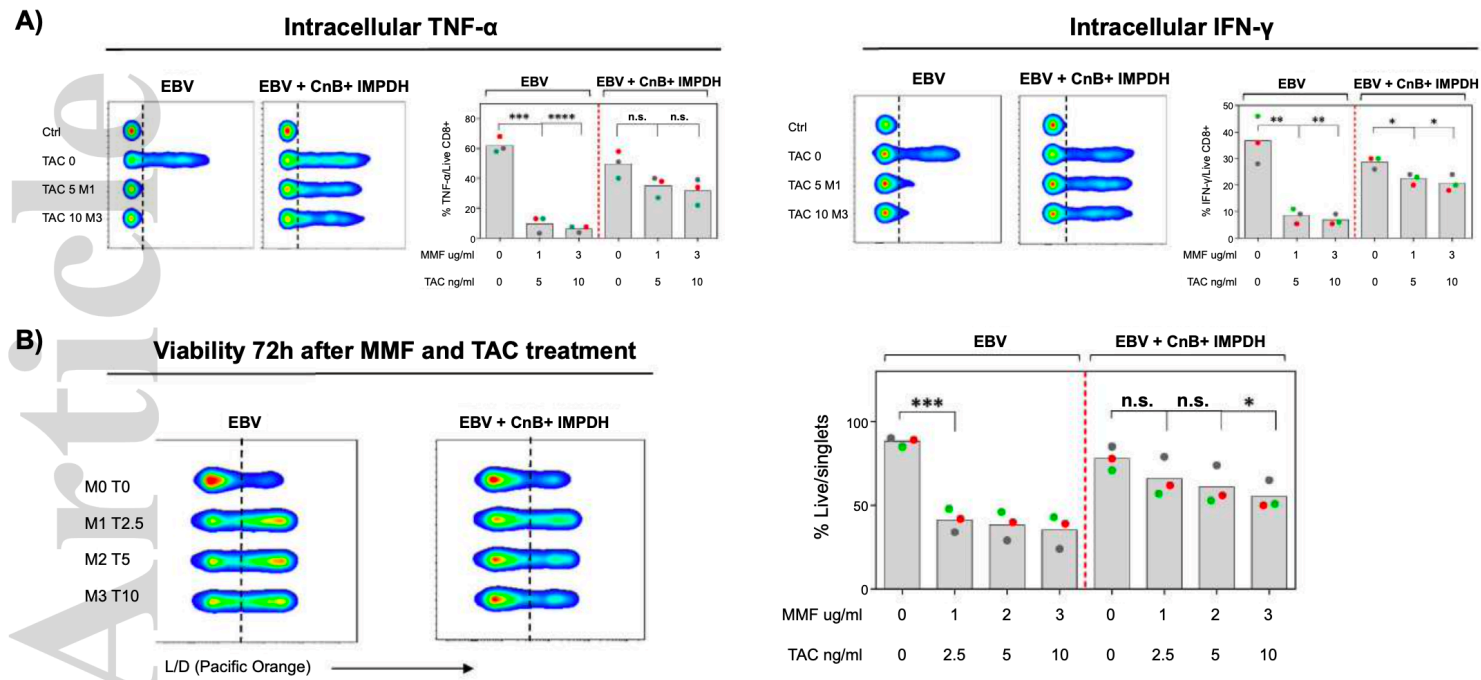


Fig. 5. Engineering IDRA EBV-specific TCR-redirection T cells. IDRA EBV TCR-T cells were developed by electroporating mRNA encoding EBV-specific TCR, mutant CnB and mutant IMPDH. Engineered T cells were co-incubated with HLA-A2+ EBV-specific peptide pulsed or non-pulsed T2 cells overnight. Intracellular cytokine staining and viability analysis were performed after the indicated time. (A) Representative experiment stained for TNF- α or IFN- γ . Bar graphs demonstrate the percentage of cytokine-positive CD8+ T cells (n = 3). DMSO-treated T cells without targets served as negative control. (B) Viability of T cell were assessed by live-dead staining after 72 hours exposure to the respective drugs. DMSO-treated T cells from same donor served as a control for viability assessment. Representative experiment stained with live/dead discrimination dye (left panel). Each dot represents one individual experiment in bar graphs. Statistical significance was evaluated by 2-tailed t test (*0.01 to 0.05, ** 0.001 to 0.01, *** 0.0001 to 0.001, **** < 0.0001, n.s., not significant).